Mesoporous Materials

International Edition: DOI: 10.1002/anie.201509054
German Edition: DOI: 10.1002/ange.201509054

No More HF: Teflon-Assisted Ultrafast Removal of Silica to Generate High-Surface-Area Mesostructured Carbon for Enhanced CO_2 Capture and Supercapacitor Performance

*Dheeraj Kumar Singh, Katla Sai Krishna, Srinivasan Harish, Srinivasan Sampath, and Muthusamy Eswaramoorthy**

Abstract: *An innovative technique to obtain high-surface-area mesostructured carbon (2545 $m^2 g^{-1}$) with significant microporosity uses Teflon as the silica template removal agent. This method not only shortens synthesis time by combining silica removal and carbonization in a single step, but also assists in ultrafast removal of the template (in 10 min) with complete elimination of toxic HF usage. The obtained carbon material (JNC-1) displays excellent CO_2 capture ability (ca. 26.2 wt% at 0°C under 0.88 bar CO_2 pressure), which is twice that of CMK-3 obtained by the HF etching method (13.0 wt%). JNC-1 demonstrated higher H_2 adsorption capacity (2.8 wt%) compared to CMK-3 (1.2 wt%) at −196°C under 1.0 bar H_2 pressure. The bimodal pore architecture of JNC-1 led to superior supercapacitor performance, with a specific capacitance of 292 $F g^{-1}$ and 182 $F g^{-1}$ at a drain rate of 1 $A g^{-1}$ and 50 $A g^{-1}$, respectively, in 1 M H_2SO_4 compared to CMK-3 and activated carbon.*

Periodic mesoporous carbon[1,2] materials have generated a great deal of technological interest by virtue of their ability to overcome the mass-transport limitations encountered in their disordered counterparts[3] and thus play a significant role in the area of catalysis (as a support),[4] Li-S batteries,[5] gas separation and storage,[6,7] and electric double-layer capacitors (EDLC).[8] In contrast to disordered pore architectures, ordered nanoporous structures provide shorter diffusion pathways and minimal resistance to molecular motion, which improves transport properties.[3] The more versatile method to synthesize ordered mesoporous carbon materials relies on the inverse replica strategy using ordered mesoporous silica as a hard template and sucrose as the inexpensive carbon precursor.[9] However, removal of the hard silica template is a bottleneck to scale up the synthesis as it involves the use of HF or repeated treatment with NaOH solution at elevated temperatures.[9] HF is highly toxic[10] and its use is highly discouraged in many countries, while NaOH treatment is time consuming, corrosive, and not-cost effective as it has to be operated at elevated temperatures.[11] Furthermore, the surface area of the ordered mesoporous carbon obtained through the hard-template method is very moderate in comparison to many high-surface-area disordered carbons.[12,13] Though a silica-free strategy to prepare mesoporous carbon was reported as an alternate method, it involves usage of corrosive and expensive carbon precursors such as phenol and formaldehyde with a polymeric template such as F127.[14] Furthermore, it suffers from significant amount of structural shrinkage during the carbonization process, resulting in low surface areas, smaller pore sizes, and reduced pore volume.[15] Thus, a simple and less hazardous approach to remove silica without the direct use of HF is much needed to make the silica template strategy as a successful method to prepare high-surface-area mesostructured carbon.

Herein, an innovative way of using Teflon powder instead of HF to etch out the silica is described in which the separate , carbonization, and silica removal are combined into one step (Scheme 1). The silica removal using Teflon is very straightforward, easy to handle (simply mixing the Teflon powder and the sample before carbonization), and extremely fast (silica removal is complete within 10 min). More importantly, the carbon thus obtained retains its mesoscale order and shows

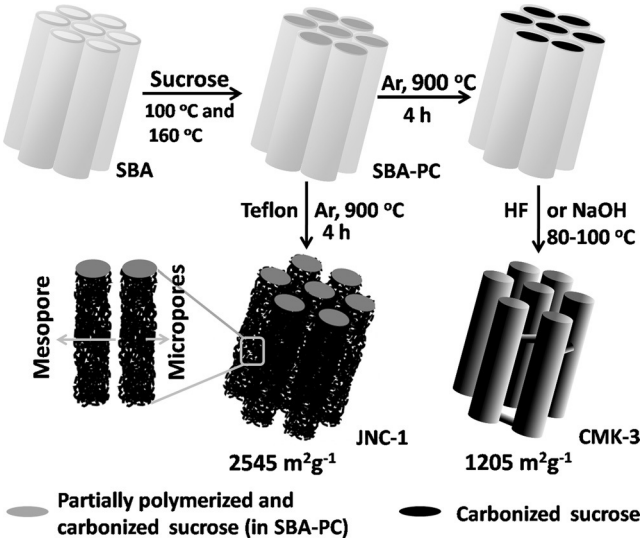

Scheme 1. Comparison of the conventional synthesis of CMK-3 with that of JNC-1.

[*] D. K. Singh, Dr. K. S. Krishna, Prof. M. Eswaramoorthy
Nanomaterials and Catalysis Lab
Chemistry and Physics of Materials Unit
Jawaharlal Nehru Centre for Advanced Scientific Research (JNCASR)
Jakkur P.O., Bengaluru 560064 (India)
E-mail: eswar@jncasr.ac.in
Dr. S. Harish, Prof. S. Sampath
Department of Inorganic and Physical Chemistry
Indian Institute of Science, Bengaluru 560012 (India)

Supporting information for this article is available on the WWW under http://dx.doi.org/10.1002/anie.201509054.

a very high surface area, which is more than two times higher than the carbon prepared by the HF etching method (Scheme 1). The obtained ordered nanoporous carbon (JNC-1) shows remarkable performance for CO_2 capture, hydrogen storage, and dye adsorption in comparison to HF etched CMK-3 carbon. It also exhibits superior performance as a supercapacitor material.

Carbonization of SBA-PC at higher temperature followed by etching of silica with corrosive HF gives CMK-3 carbon (Scheme 1; Supporting Information, Figure S3), an inverse replica of SBA[16] (Supporting Information, Figure S2). In a significant deviation from the conventional two-step process we simply mixed the SBA-PC with Teflon powder and heated to 900 °C for 4 h (Scheme 1) in Ar. The process combines the carbonization and silica removal in a single step with complete elimination of toxic HF usage. The carbon replica of SBA thus obtained is named JNC-1 (Scheme 1, Figure 1 a; Supporting Information, Figure S4). Mesostructured carbon

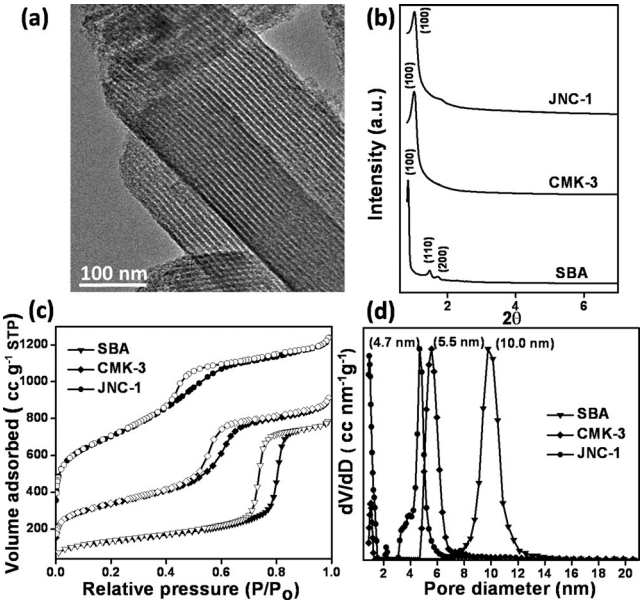

Figure 1. a) TEM image of JNC-1. b) PXRD patterns, c) N_2 adsorption (closed symbols)–desorption isotherms (open symbols) and d) corresponding pore size distributions (normalized, calculated using NLDFT/QSDFT method) of SBA, CMK-3, and JNC-1.

CMK-3 was also made from the same SBA-PC through the standard two-step process involving carbonization at high temperature (900 °C for 4 h) followed by HF etching (12 h at room temp) (Supporting Information, Figure S3) of silica for comparison as reported by Jun et al.[9]

The powder X-ray diffraction (PXRD) pattern of SBA (Figure 1 b) shows characteristic low-angle peaks for mesostructured materials having a *p6mm* honeycomb lattice symmetry.[17] JNC-1 exhibits well-resolved low-angle peaks, as that of CMK-3 (Figure 1 b), which can be indexed as (100), (110), and (200) indicating faithful negative replication of mesostructural ordering of parent SBA.[9] Wide-angle PXRD pattern of JNC-1 (Supporting Information, Figure S5) showed broad diffraction peaks around 22° and 43° (2θ), indicating amorphous nature of the carbon walls,[18] similar to that of activated carbon (AC) and CMK-3, which was further confirmed by the observation of higher intensity D band (I_D) compared to the G band (I_G) in the Raman spectra (Supporting Information, Figure S6).[19] The absence of a Si peak in energy-dispersive X-ray spectroscopy (EDS) analyses of JNC-1 carbon shows the complete removal of silica template (Supporting Information, Figure S7a). A transmission electron microscope (TEM) image of JNC-1 (Figure 1 a) indicates well-aligned mesochannels similar to that of CMK-3 (Supporting Information, Figure S3), the exact negative replica of SBA-15 (Supporting Information, Figure S2). N_2 adsorption–desorption isotherms of SBA (Figure 1 c) exhibit type IV behavior characteristic of mesoporous materials[20] with a capillary condensation at around P/P_o of 0.75. The surface area of JNC-1 was found to be around 2545 $m^2 g^{-1}$, which is twice to that of CMK-3 (1205 $m^2 g^{-1}$; Supporting Information, Table S2). It must be mentioned that the standard BET method for the calculation of surface area of micro-mesostructured materials is not applicable here and hence the criteria suggested by Rouquerol et al.[21] has been used for the calculation of surface areas (Supporting Information, Figure S8). Hysteresis loops of JNC-1 and CMK-3 (Figure 1 c) exhibit H2 type characteristics with the effect being more pronounced for JNC-1, indicating the presence of significant amount of micropores.[9] Pore size distribution of SBA (Figure 1 d) was calculated by NLDFT method whereas QSDFT was implemented for the calculation of pore sizes for JNC-1 and CMK-3 (Figure 1 d), as it takes into account the nature of surface geometrical heterogeneity than merely treating the walls as a featureless plane surface as in NLDFT and hence is more accurate.[22] In contrast to CMK-3, JNC-1 shows bimodal pore-size distribution (Figure 1 d) having meso- and micropores with average pore diameters centered at 4.7 nm and 0.9 nm, respectively. As compared to CMK-3, JNC-1 shows significant amount of micropores indicated by very sharp N_2 uptake at very low pressure (Figure 1 c) owing to the presence of abundant micropores of sizes about 0.9 nm (Figure 1 d). The t-plot analyses[23,24] of JNC-1 indicate the presence of considerable fraction of microporous surface area (1012 $m^2 g^{-1}$; Supporting Information, Table S2) and micropore volume (0.43 cc g^{-1}) as compared to CMK-3 (370 $m^2 g^{-1}$, 0.16 cc g^{-1}; Supporting Information, Table S2). Furthermore, micropore analyses of JNC-1 and CMK-3 via CO_2 sorption at 0 °C indicate the presence of significant amount of micropores with a pore size of circa 0.8 nm in the former (Supporting Information, Figure S9).

Control experiments of silica (SBA) performed with Teflon and polyvinylidene fluoride (PVDF) suggests that silica removal occurs through the formation of SiF_4 by reaction of silica with in situ generated HF in the presence of partially polymerized sucrose carbon (see the Supporting Information, Figure S10–S12 and discussions therein).[25] Thermogravimetric analysis (TGA) shows that Teflon starts to decompose in an inert environment (N_2) at 450 °C and completes at 560 °C (Supporting Information, Figure S10b).[26] When SBA-PC was mixed with Teflon and heated at 650 °C (with a heating rate 5 °C min^{-1} from room temperature) in Ar for 10 min, entire silica was removed as evident from EDS

analyses (Supporting Information, Figure S13a). Furthermore, the obtained material (JNC_{650}) shows 13 wt% oxygen content (Supporting Information, Figure S13a), due to incomplete carbonization as compared to 3 wt% oxygen obtained for JNC-1 (Supporting Information, Figure S7a). PXRD pattern of JNC_{650} (Supporting Information, Figure S14) also exhibits the low angle peaks corresponding to the mesoscale ordering. This suggests that the mesostructure is preserved, notwithstanding the silica removal even before complete carbonization occurs (Supporting Information, Figures S16, S17). The specific surface area is 1204 $m^2 g^{-1}$, which is equivalent to CMK-3 as well as the mesoporous carbon (1184 $m^2 g^{-1}$) obtained through similar carbonizing condition (650 °C–10 min) but with HF etching (CMK_{650}; Supporting Information, Table S3 and Figure S15). Interestingly, subsequent heating of the silica free JNC_{650} and CMK_{650} in Ar at 900 °C for 4 h, referred to as JNC_{650}-900 and CMK_{650}-900 respectively, showed notable improvement in their surface areas (2459 $m^2 g^{-1}$ for JNC_{650}-900 and 2113 $m^2 g^{-1}$ for CMK_{650}-900) and total pore volume (Supporting Information, Table S3, Figures S16–S19), which is possibly due to the creation of additional pores by the removal of volatile oxygen-containing moieties upon further pyrolysis.[27,28] Mesoscale ordering of JNC_{650}-900 and CMK_{650}-900 was confirmed by low-angle PXRD peaks (Supporting Information, Figures S14, S15). This is in contrast to the relatively low surface area obtained for CMK-3 (Supporting Information, Table S2), where the silica was removed after the SBA-PC composite was carbonized at 900 °C for 4 h. The CMK-3 heated again in argon atmosphere at 900 °C for 4 h (CMK-3-900) gives a significant increase in surface area to 2548 $m^2 g^{-1}$ (Supporting Information, Table S4, Figures S20, S21). This clearly suggests that presence of silica impede the development of micropores by forming stable silica–carbon interface, thus inhibiting the thermal decomposition of surface carbon at 900 °C, which was facilitated when the silica free carbons (CMK-3, JNC_{650} and CMK_{650}) were heated at 900 °C in Ar for 4 h. When SBA-PC composite is mixed with Teflon and slowly heated in an argon environment, simultaneous carbonization and silica removal occurs within 650 °C, and further raise in temperature expedites the removal of volatile oxygenated moieties[27,28] and hence the formation of micropores, leading to a high-surface-area ordered carbon structure in a single step. In the case of CMK-3, the presence of a silica–carbon interface during carbonization (at 900 °C) inhibits such a mechanism, resulting in a relatively low surface area. The carbon replica (JNC-2) obtained through the analogous procedure using mesoporous silica KIT-6[29] template also shows high surface area when the silica was removed by Teflon (Supporting Information, Figures S22–S26 and Table S5).

The influence of bimodal (micro-meso) pore-size distribution of JNC-1 on the sorption behavior of organic pollutants was investigated using two synthetic azo dyes of different sizes (Alizarin Yellow, size 1.3 nm and Congo Red, size ca. 2.6 nm).[30] The sorption performance of JNC-1 was compared with the CMK-3 (mesoporous) and activated carbon (AC).Liquid phase dye adsorption studies indicate very high uptake of Congo red and Alizarin yellow over JNC-1 in comparison to CMK-3 and AC (Figure 2a–c; Supporting Information, Figure S27). Such a superior dye uptake of JNC-1 can be explained by bimodal pore size distribution in JNC-1, avoiding mass-transfer limitations encountered in narrow micropores and a high surface area.

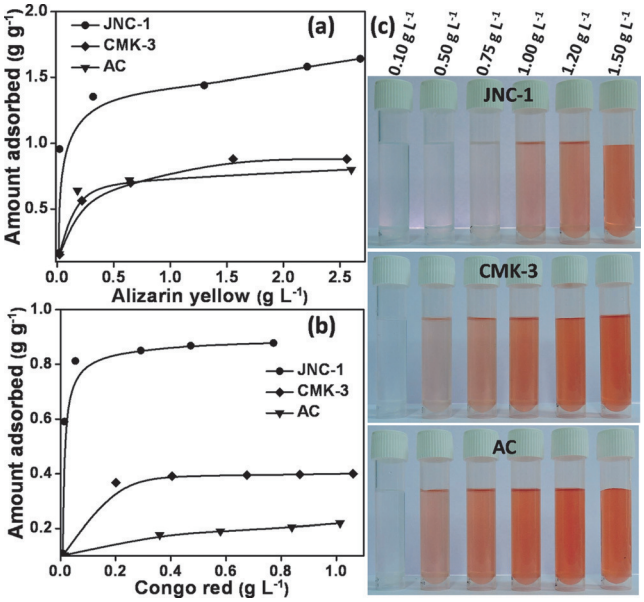

Figure 2. Adsorption isotherms of a) Alizarin yellow and b) Congo red over JNC-1, CMK-3, and AC. c) Optical images of Congo red adsorption by different carbon materials (concentrations at the top of Figure 2c are initial concentrations with an equal amount of different adsorbents added in each case).

Furthermore, carbon dioxide and hydrogen sorption measurements were performed to evaluate the gas storage properties of JNC-1 on account of the bimodal pore size distribution. The uptake of CO_2 and H_2 in lightweight, porous carbon materials is all the more important as the former (CO_2) being a greenhouse gas needs to be sequestered from the air or industry effluents and the latter (H_2) is an important source for clean energy but needs to be stored in a material for the safe and efficient usage. JNC-1 showed a very high uptake for CO_2 of around 154 wt% at −78 °C (0.88 bar) as compared to 73 wt% over CMK-3 under similar conditions (Figure 3b). Even at 0 °C and 25 °C (under 0.88 bar of CO_2 pressure) the CO_2 sorption on JNC-1 was found to be around 26 wt% and 15 wt% respectively (Figure 3c), which are significantly higher than those of CMK-3, whose sorption capacity were determined to be 13 wt% and 7 wt% at 0 °C and 25 °C, respectively (Figure 3d). Such exceptional CO_2 uptake (Supporting Information, Table S6) can be attributed to unique textural parameters of JNC-1.[31] The uptake for CO_2 at 25 °C (1 bar) over JNC-1 remains the same even after 10 cycles (Supporting Information, Figure S28). The selectivity for CO_2/N_2 separation (calculated from ratio of initial slopes) over JNC-1 at 25 °C was found to be about 7 compared to 6 of CMK-3 and can be attributed to the presence of abundant micropores (Supporting Information, Figure S29) in the former.[6,32,33] Hydrogen uptake (2.8 wt%) of JNC-1 at

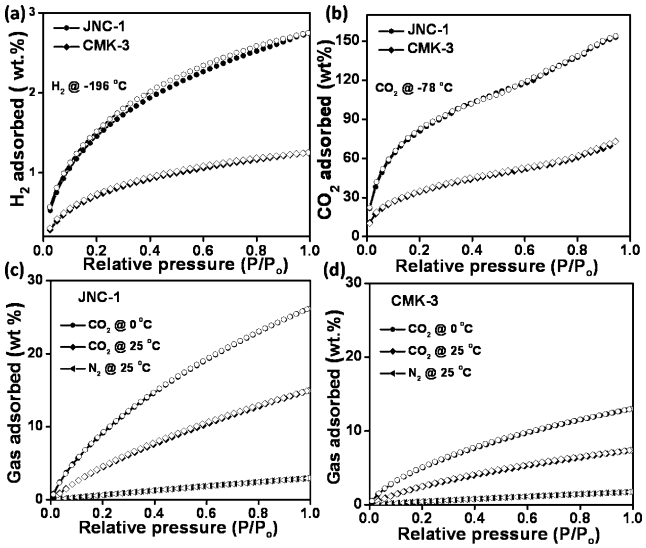

Figure 3. a) H_2 and b) CO_2 adsorption isotherms of JNC-1 and CMK-3 at −196 °C and −78 °C, respectively. c), d) CO_2 adsorption isotherms (at 0 °C and 25 °C) along with N_2 adsorption isotherm (at 25 °C) of c) JNC-1 and d) CMK-3. (Note: closed and open symbols represent adsorption and desorption points. P_o for N_2 and CO_2 isotherms is taken as 660 torr (0.88 bar) whereas for H_2 it is 760 torr (1.01 bar)).

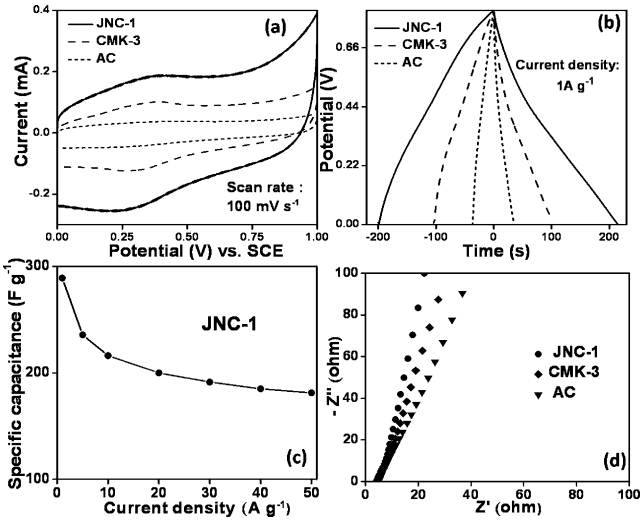

Figure 4. Comparison of electrochemical performances of JNC-1 with CMK-3 and AC. a) Cyclic voltammetry (CV) curves (scan rate: 100 mV s^{-1}) and b) galvanostatic charge–discharge (CD) profiles at a current density of 1 A g^{-1} of JNC-1, CMK-3, and AC in 1 M H_2SO_4. c) Rate capability performance of JNC-1 and d) Nyquist plot of different carbon materials studied, depicting an ideal capacitor type of behavior for JNC-1.

−196 °C (1.0 atm; Figure 3a) was also found to be higher than that of CMK-3 (1.2 wt %; Figure 3a; Supporting Information, Table S7) and is completely reversible throughout the pressure range studied. The presence of huge amount of micropores (40 %) having a size of about 0.9 nm is within the accepted range of optimum micropore diameter for hydrogen storage (that is, between 0.5–1.5 nm) and contributes as sites of high energy of adsorption, thereby maximizing the uptake.[34,35] On the other hand, CMK-3 obtained through HF etching shows negligible H_2 uptake due to lack of enhanced microporosity.[36]

Electrochemical performances of JNC-1, CMK-3, and AC were evaluated through cyclic voltammetry (CV), galvanostatic charge/discharge (CD), and electrochemical impedance spectroscopy (EIS) studies using a typical three-electrode setup. The CV curve of JNC-1 is pseudo rectangular in shape (Figure 4a), indicating a capacitive type of behavior at the scan rate of 100 mV s^{-1}. As the scan rate is increased up to 2 V s^{-1}, cyclic voltammograms still retain the rectangular shape (Supporting Information, Figure S30), indicating fast charge–discharge and the high power capability of the JNC-1.[37] The galvanostatic CD curve of JNC-1 is triangular in nature (Figure 4b), which further confirms efficient ion transport without significant IR drop. The JNC-1 carbon exhibited specific capacitance of around 274 F g^{-1} at 1 A g^{-1} and value was retained till several cycles as compared to 132 F g^{-1} and 49 F g^{-1} for CMK-3 and AC, respectively, at the same current density (Supporting Information, Figure S31). In fact, in one of the batches, a specific capacitance value of 292 F g^{-1} at 1 A g^{-1} (Figure 4c) was found and is one of the best reported values for pure carbon based materials (Supporting Information, Table S8).[38,39] Additionally, JNC-1 exhibits excellent cyclic stability over studied 1200 cycles at 10 A g^{-1}, retaining 98 % of the original capacity (Supporting Information, Figure S32). The rate capability performance of JNC-1 indicate a retention of specific capacitance of around 213 F g^{-1} and 180 F g^{-1} at 10 A g^{-1} and 50 A g^{-1}, respectively (Figure 4c). To the best of our knowledge these values are one of the highest at such high drain rates for pure carbon-based materials.[38,39] In comparison to CMK-3 and AC, a Nyquist plot of JNC-1 is almost vertical to the imaginary axis (Figure 4d), signifying the performance tending to that of an ideal capacitor, as ion migration are not hindered.[40] Mesopores help in attaining high capacitance values at a higher drain rate by the rapid supply of ions to the active electrode interface, which is not possible in a purely microporous sample on account of the limited space available for ion transport. Such performance metrics can be traced back to highly connected bimodal pore size distribution of JNC-1, exhibiting a synergistic effect of facilitating efficient charge transfer (mesopores) process and enhanced electric double-layer formation (micropores).[12,37] In other words, the presence of huge amount micropores in JNC-1 contribute towards high-energy density, and an equally large extent of mesopores aid towards enhanced power density.[12,37]

In conclusion, use of Teflon not only eliminates the handling of toxic HF or repeated NaOH washes but also drastically reduces the time required for mesopore carbon generation, as it combines the carbonization and template removal step as a single step. Moreover, the obtained carbon material, JNC-1, exhibits superior supercapacitor performance, and the capacitance values are one of the highest reported for such ordered carbon materials at such a higher drain rate. Furthermore, JNC-1 exhibits excellent dye adsorption and exceptional gas storage properties (H_2 and

CO_2) compared to CMK-3, which is comparable to most of the best reported MOFs.

Acknowledgements

We thank Prof. C. N. R. Rao for his constant encouragement and support. D.K.S. thanks the CSIR for a fellowship. D.K.S. also thanks Jiaul Hoque for dye adsorption measurements and Sujoy Sarkar for electrochemical measurements.

Keywords: gas storage · ordered mesoporous carbons · silica · supercapacitors · Teflon

How to cite: *Angew. Chem. Int. Ed.* **2016**, *55*, 2032–2036
Angew. Chem. **2016**, *128*, 2072–2076

[1] R. Ryoo, S. H. Joo, M. Kruk, M. Jaroniec, *Adv. Mater.* **2001**, *13*, 677–681.
[2] J. Lee, J. Kim, T. Hyeon, *Adv. Mater.* **2006**, *18*, 2073–2094.
[3] A. Walcarius, *Chem. Soc. Rev.* **2013**, *42*, 4098–4140.
[4] S. H. Joo, S. J. Choi, I. Oh, J. Kwak, Z. Liu, O. Terasaki, R. Ryoo, *Nature* **2001**, *412*, 169–172.
[5] X. Ji, K. T. Lee, L. F. Nazar, *Nat. Mater.* **2009**, *8*, 500–506.
[6] J. Zhang, Z.-A. Qiao, S. M. Mahurin, X. Jiang, S.-H. Chai, H. Lu, K. Nelson, S. Dai, *Angew. Chem. Int. Ed.* **2015**, *54*, 4582–4586; *Angew. Chem.* **2015**, *127*, 4665–4669.
[7] M. Choi, R. Ryoo, *J. Mater. Chem.* **2007**, *17*, 4204–4209.
[8] J. Wei, D. Zhou, Z. Sun, Y. Deng, Y. Xia, D. Zhao, *Adv. Funct. Mater.* **2013**, *23*, 2322–2328.
[9] S. Jun, S. H. Joo, R. Ryoo, M. Kruk, M. Jaroniec, Z. Liu, T. Ohsuna, O. Terasaki, *J. Am. Chem. Soc.* **2000**, *122*, 10712–10713.
[10] J. C. Bertolini, *J. Emerg. Med.* **1992**, *10*, 163–168.
[11] J. Li, Y. Liang, B. Dou, C. Ma, R. Lu, Z. Hao, Q. Xie, Z. Luan, K. Li, *Mater. Chem. Phys.* **2013**, *138*, 484–489.
[12] M. Karthik, E. Redondo, E. Goikolea, V. Roddatis, S. Doppiu, R. Mysyk, *J. Phys. Chem. C* **2014**, *118*, 27715–27720.
[13] J. Pang, X. Li, D. Wang, Z. Wu, V. T. John, Z. Yang, Y. Lu, *Adv. Mater.* **2004**, *16*, 884–886.
[14] Y. Meng, D. Gu, F. Zhang, Y. Shi, H. Yang, Z. Li, C. Yu, B. Tu, D. Zhao, *Angew. Chem. Int. Ed.* **2005**, *44*, 7053–7059; *Angew. Chem.* **2005**, *117*, 7215–7221.
[15] R. Liu, Y. Shi, Y. Wan, Y. Meng, F. Zhang, D. Gu, Z. Chen, B. Tu, D. Zhao, *J. Am. Chem. Soc.* **2006**, *128*, 11652–11662.
[16] D. Zhao, J. Feng, Q. Huo, N. Melosh, G. H. Fredrickson, B. F. Chmelka, G. D. Stucky, *Science* **1998**, *279*, 548–552.
[17] A. Sayari, B.-H. Han, Y. Yang, *J. Am. Chem. Soc.* **2004**, *126*, 14348–14349.
[18] Y. Xia, R. Mokaya, *Adv. Mater.* **2004**, *16*, 1553–1558.
[19] T.-W. Kim, I.-S. Park, R. Ryoo, *Angew. Chem. Int. Ed.* **2003**, *42*, 4375–4379; *Angew. Chem.* **2003**, *115*, 4511–4515.
[20] K. S. W. Sing, D. H. Everett, R. A. W. Haul, L. Moscou, R. A. Pierotti, J. Rouquerol, T. Siemieniewska, *Pure Appl. Chem.* **1985**, *57*, 603–619.
[21] J. Rouquerol, P. Llewellyn, F. Rouquerol in *Studies in Surface Science and Catalysis*, *Vol. 160* (Eds.: F. R.-R. J. R. P. L. Llewellyn, N. Seaton), Elsevier, **2007**, pp. 49–56.
[22] A. V. Neimark, Y. Lin, P. I. Ravikovitch, M. Thommes, *Carbon* **2009**, *47*, 1617–1628.
[23] B. C. Lippens, J. H. de Boer, *J. Catal.* **1965**, *4*, 319–323.
[24] S. Lowell, J. E. Shields, M. A. Thomas, M. Thommes, *Characterization of Porous Solids and Powders: Surface Area*, *Pore Size and Density*, Springer, Amsterdam, **2012**.
[25] S. L. Madorsky, V. E. Hart, S. Straus, V. A. Sedlak, *J. Res. Natl. Bur. Stand.* **1953**, *51*, 327–333, Research Paper No. 2461.
[26] J. A. Conesa, R. Font, *Polym. Eng. Sci.* **2001**, *41*, 2137–2147.
[27] P. F. Nelson, I. W. Smith, R. J. Tyler, J. C. Mackie, *Energy Fuels* **1988**, *2*, 391–400.
[28] A.-H. Lu, D. Zhao, Y. Wan, *Nanocasting: a versatile strategy for creating nanostructured porous materials*, Royal Society of Chemistry, Cambridge, **2010**.
[29] F. Kleitz, S. Hei Choi, R. Ryoo, *Chem. Commun.* **2003**, 2136–2137.
[30] K. K. R. Datta, D. Jagadeesan, C. Kulkarni, A. Kamath, R. Datta, M. Eswaramoorthy, *Angew. Chem. Int. Ed.* **2011**, *50*, 3929–3933; *Angew. Chem.* **2011**, *123*, 4015–4019.
[31] G. Srinivas, V. Krungleviciute, Z.-X. Guo, T. Yildirim, *Energy Environ. Sci.* **2014**, *7*, 335–342.
[32] L. K. C. de Souza, N. P. Wickramaratne, A. S. Ello, M. J. F. Costa, C. E. F. da Costa, M. Jaroniec, *Carbon* **2013**, *65*, 334–340.
[33] R. Banerjee, H. Furukawa, D. Britt, C. Knobler, M. O'Keeffe, O. M. Yaghi, *J. Am. Chem. Soc.* **2009**, *131*, 3875–3877.
[34] B. Kuchta, L. Firlej, A. Mohammadhosseini, M. Beckner, J. Romanos, P. Pfeifer, *J. Mol. Model.* **2013**, *19*, 4079–4087.
[35] Y. Xia, Z. Yang, Y. Zhu, *J. Mater. Chem. A* **2013**, *1*, 9365–9381.
[36] M. Jordá-Beneyto, F. Suárez-García, D. Lozano-Castelló, D. Cazorla-Amorós, A. Linares-Solano, *Carbon* **2007**, *45*, 293–303.
[37] K. Xia, Q. Gao, J. Jiang, J. Hu, *Carbon* **2008**, *46*, 1718–1726.
[38] Y. B. Tan, J.-M. Lee, *J. Mater. Chem. A* **2013**, *1*, 14814–14843.
[39] X.-L. Wu, A.-W. Xu, *J. Mater. Chem. A* **2014**, *2*, 4852–4864.
[40] C. Liu, Z. Yu, D. Neff, A. Zhamu, B. Z. Jang, *Nano Lett.* **2010**, *10*, 4863–4868.

Received: September 27, 2015
Revised: November 10, 2015
Published online: January 6, 2016

